

Supporting Information

Highly reversible Li_2RuO_3 cathodes in sulfide-based all solid-state lithium batteries

Yuqi Wu,^{†[a](#)} Ke Zhou,^{†[b,c](#)} Fucheng Ren,^a Yang Ha,^d Ziteng Liang,^b Xuefan Zheng,^a Zhenyu Wang,^e Wu Yang,^a Maojie Zhang,^b Mingzeng Luo,^b Corsin Battaglia,^c Wanli Yang,^d Lingyun Zhu,^e Zhengliang Gong*^a and Yong Yang*^{a,b}

^a College of Energy, Xiamen University, Xiamen 361102, China

E-mail: zlgong@xmu.edu.cn; yyang@xmu.edu.cn

^b State Key Laboratory for Physical Chemistry of Solid Surfaces, and Department of Chemistry, College of Chemistry and Chemical Engineering, Xiamen University, Xiamen 361005, China

^c Empa, Swiss Federal Laboratories for Materials Science and Technology, Dübendorf 8600, Switzerland

^d Advanced Light Source, Lawrence Berkeley National Laboratory, Berkeley, CA 94720, USA

^e Guilin Electrical Equipment Scientific Research Institute Co., Ltd, Guilin 541004, China

† These authors contributed equally.

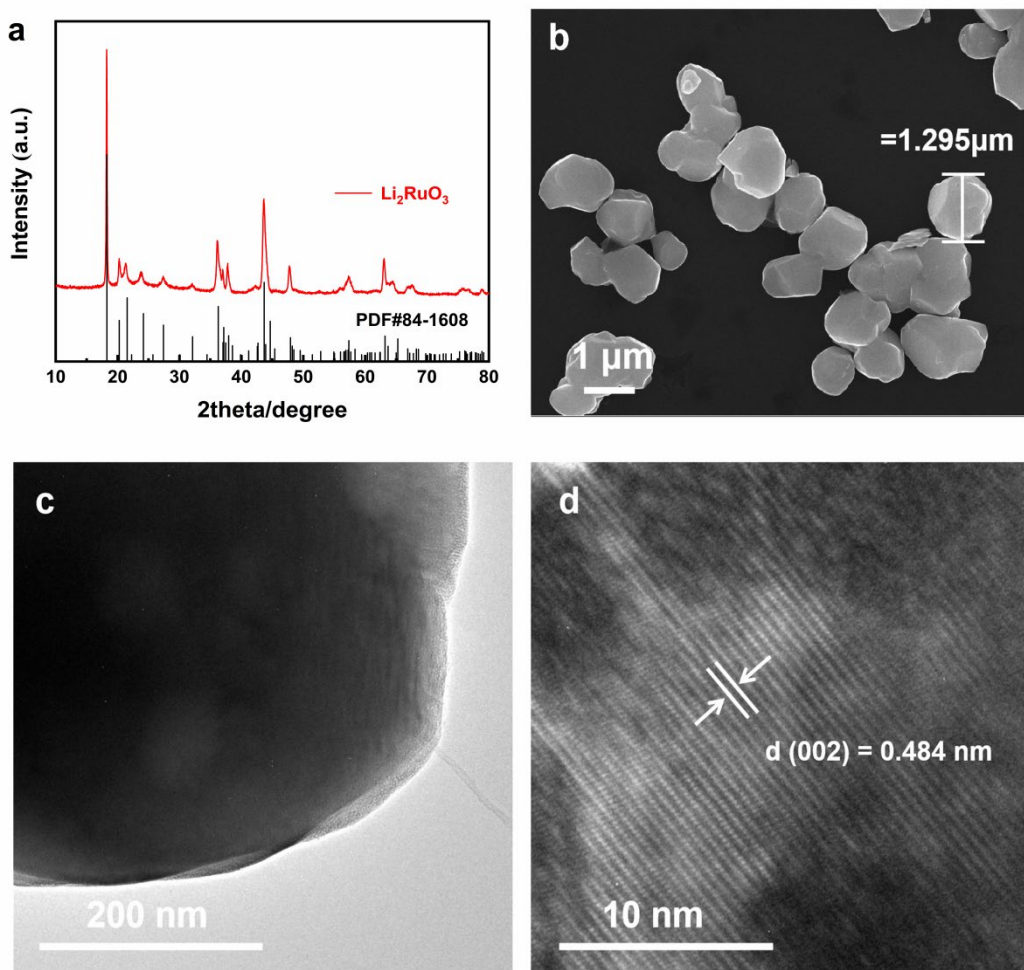


Fig. S1 The structure and morphology characterizations of the LRO. (a) XRD pattern; (b) Typical SEM image of LRO powders; (c, d) HRTEM images of LRO.

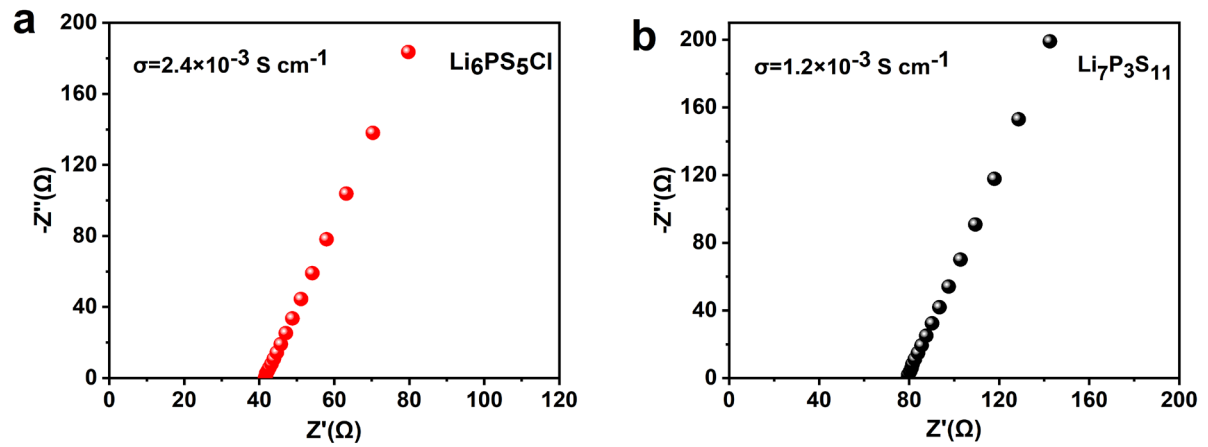


Fig. S2 EIS plots of LPSCl (a) and LPS (b) measured at room temperature.

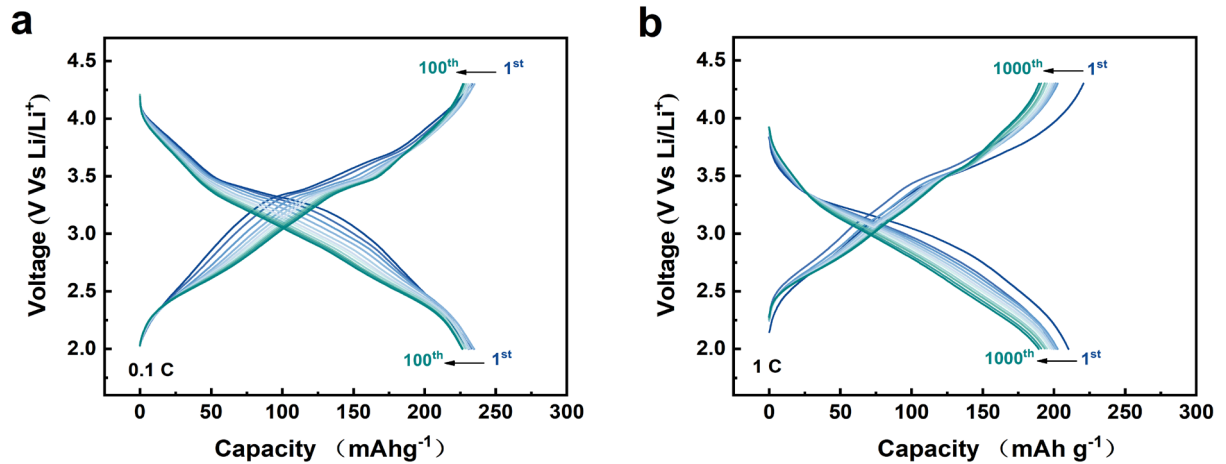


Fig. S3 The voltage profiles of LRO in ASSLBs cycled between 2.0 and 4.3 V with current 0.1C (a) and 1C (b).

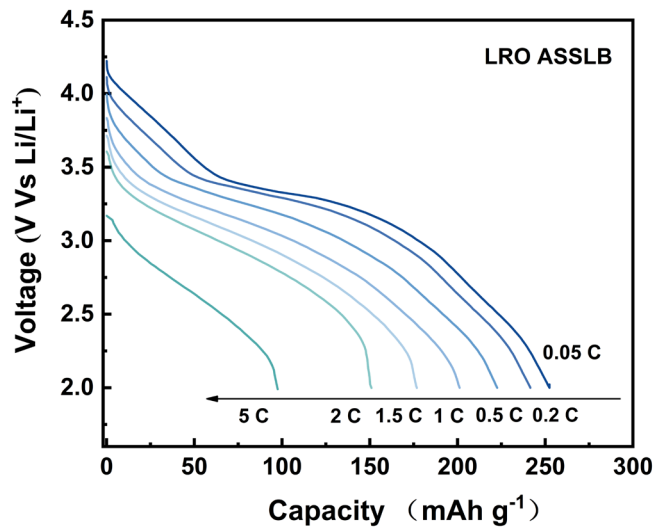


Fig. S4 Discharge voltage curves of LRO in ASSLBs at different current densities.

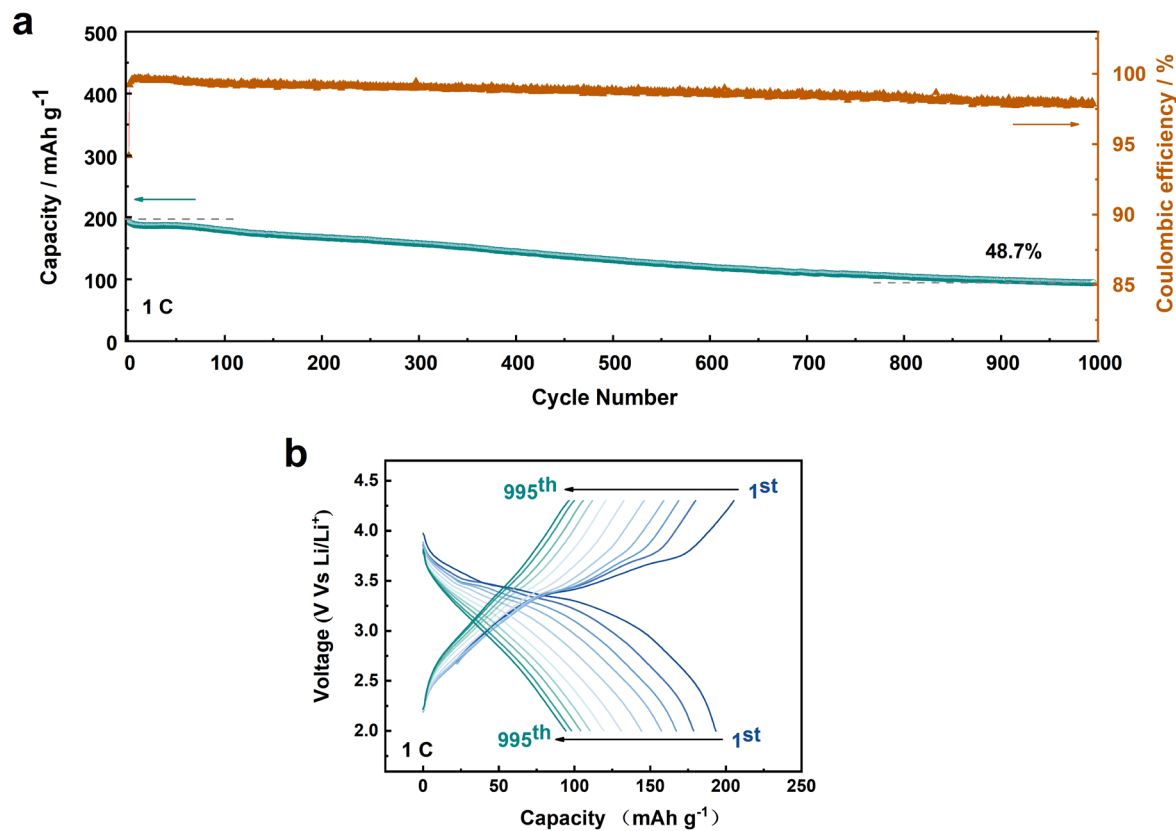


Fig. S5 (a) Cycling stability curves of LRO cathodes in LIBs at 1C with 1000 cycles between 2.0-4.3V. Before official cycling, the cells first precycled at low current density of 0.05C at 30°C for 5 cycles. (b) The corresponding voltage profiles of LRO in LIBs cycled between 2.0 and 4.3 V at 1C.

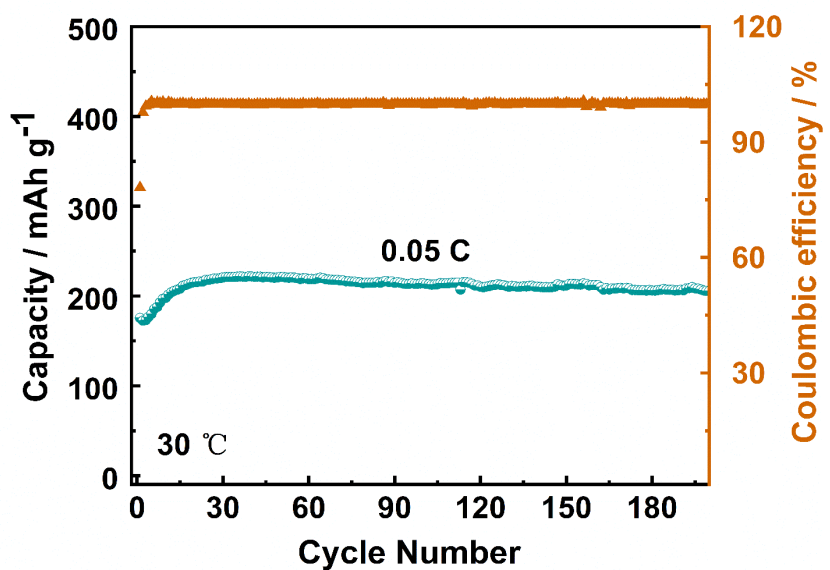


Fig. S6 Cycling performance of LRO in ASSLBs at 30 °C.

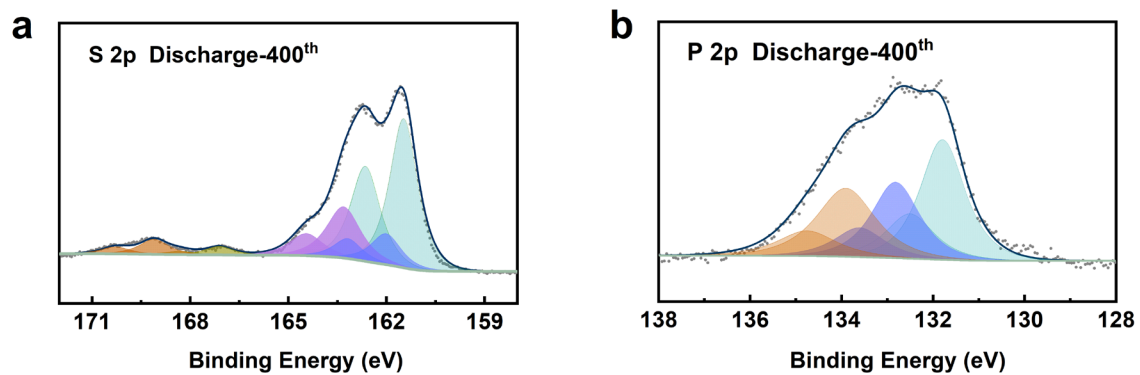


Fig. S7 S 2p (a) and P 2p (b) XPS spectra of LRO cathodes after 400 cycles.

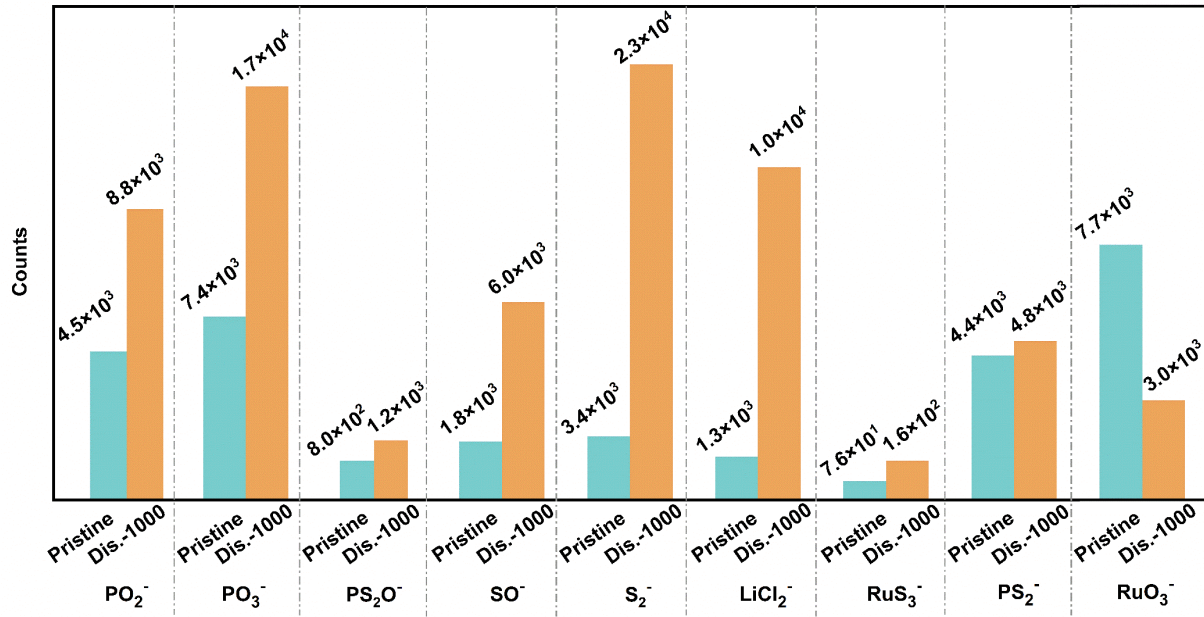


Fig. S8 Comparison of Tof-SIMS results of LRO electrodes at pristine and after 1000 cycles. “Dis.-1000” represents 1000th discharged state.

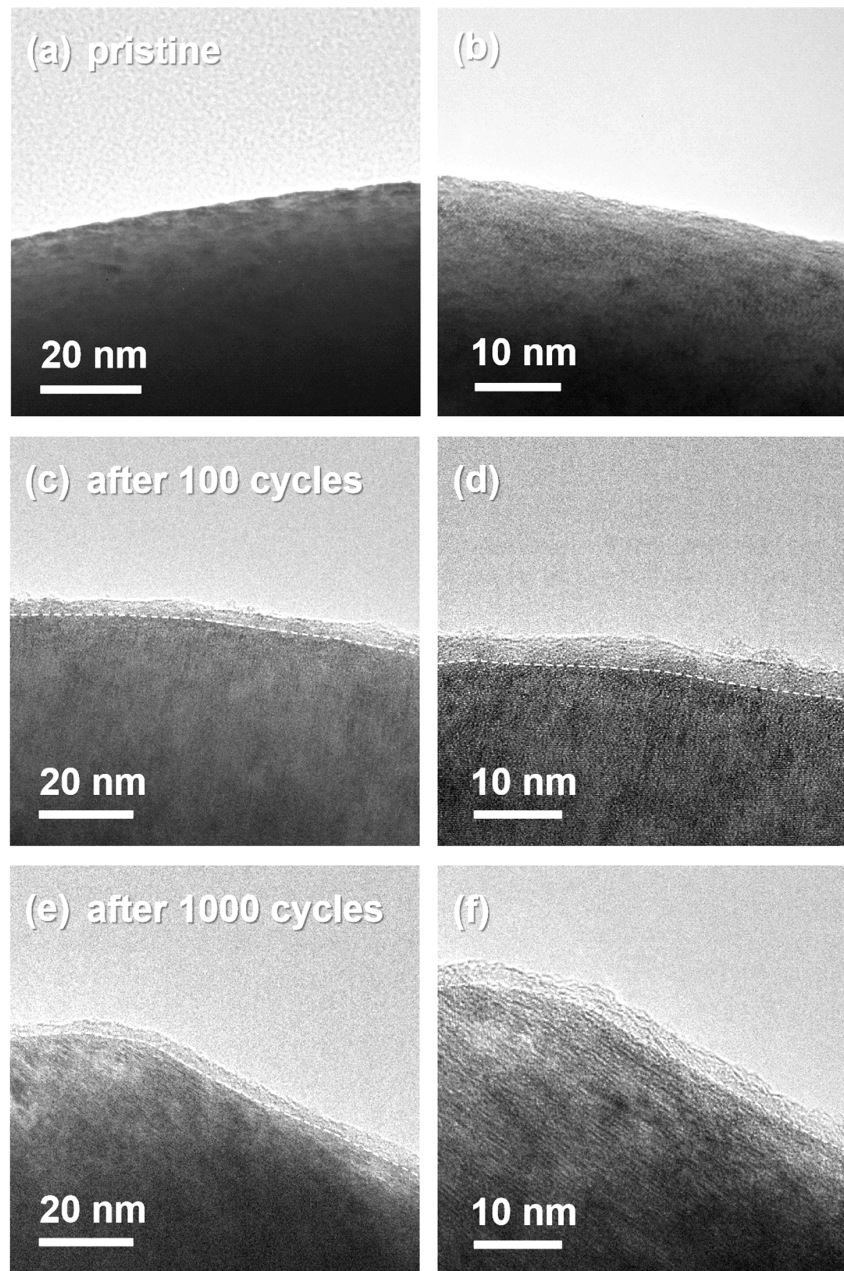


Fig.S9 TEM images of LRO particle and electrodes after cycles in ASSLBs. (a, b) at pristine, (c, d) after 100 cycles, (e, f) after 1000 cycles.

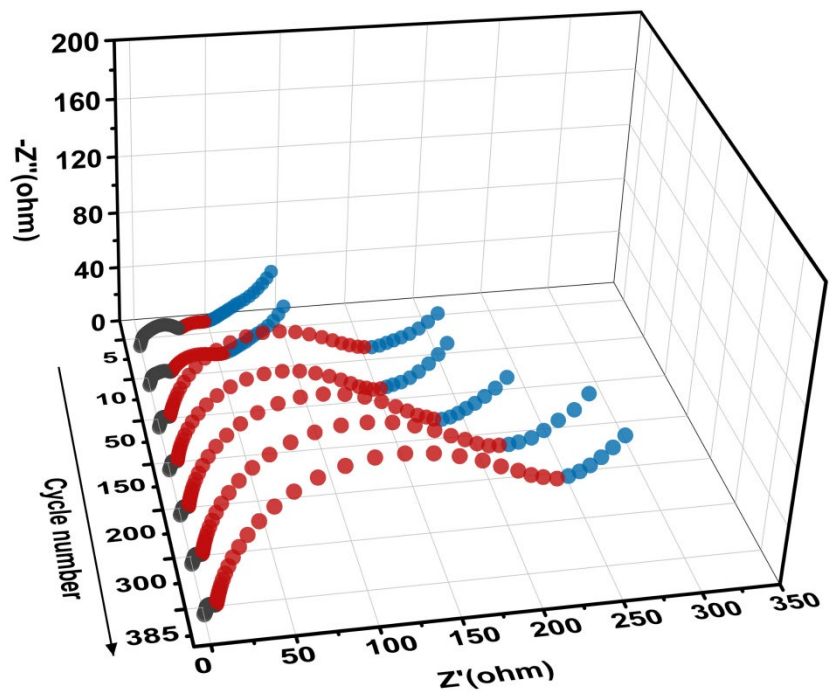


Fig. S10 Nyquist plot of the impedance spectrum during the LRO LIBs cycling.

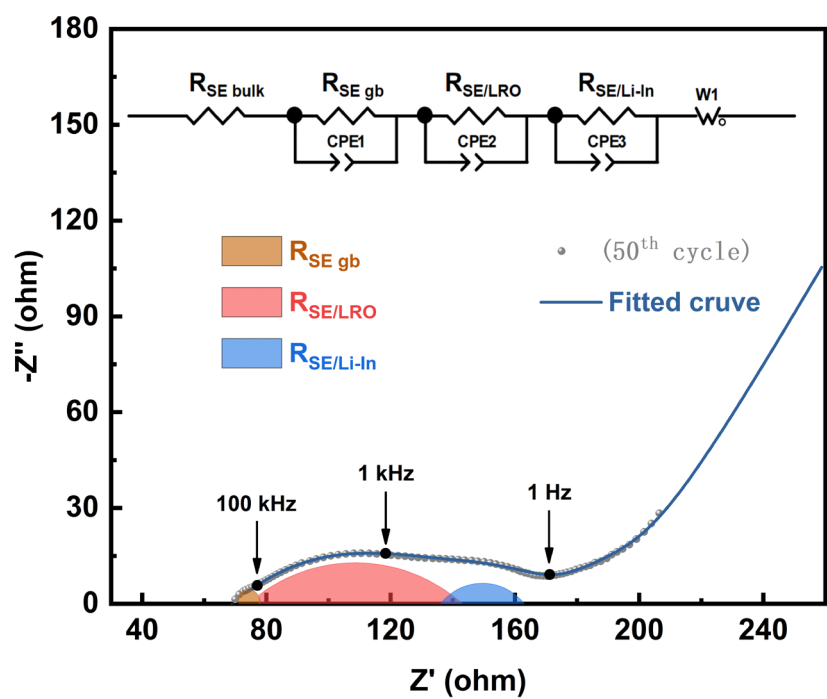


Fig. S11 A typical impedance spectra model (Nyquist plot) of the ASSLBs during cycling.

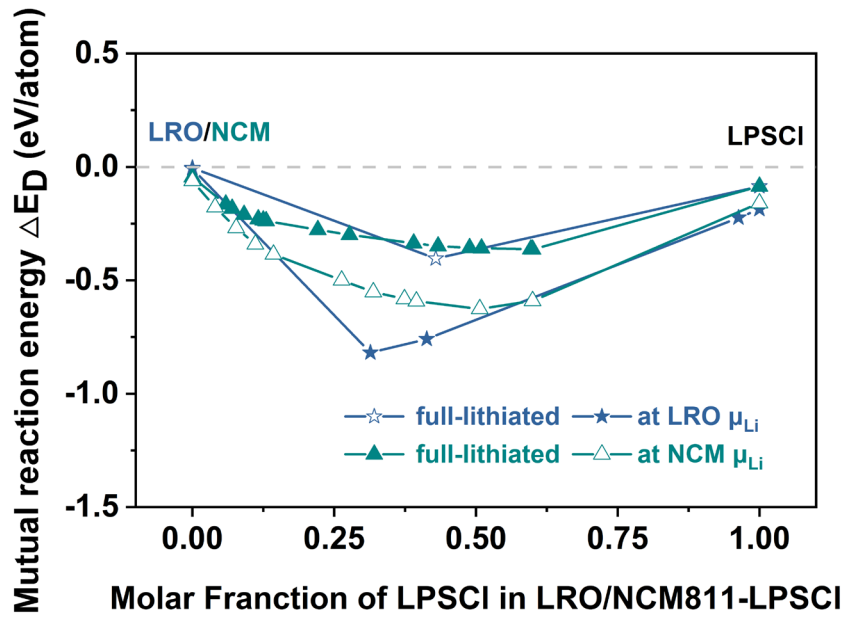


Fig. S12 The mutual reaction energy of the interface between LPSCI and LRO/NCM.

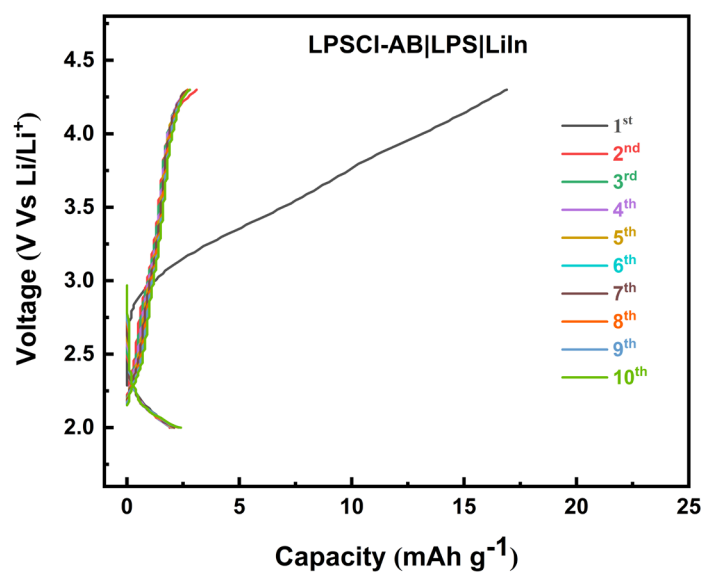


Fig. S13 Voltage profiles of the LPSCI-AB composite electrodes under the same test conditions as LRO ASSLBs.

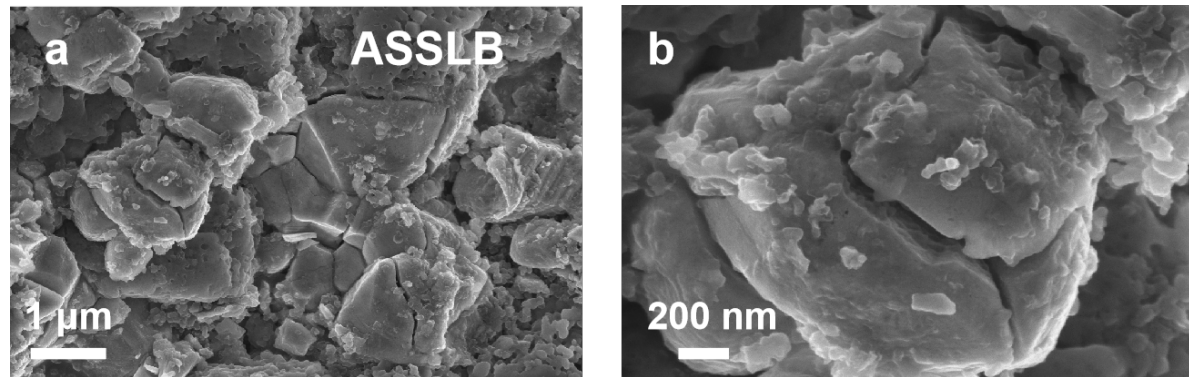


Fig. S14 The SEM images of LRO electrodes after 300 cycles in ASSLB.

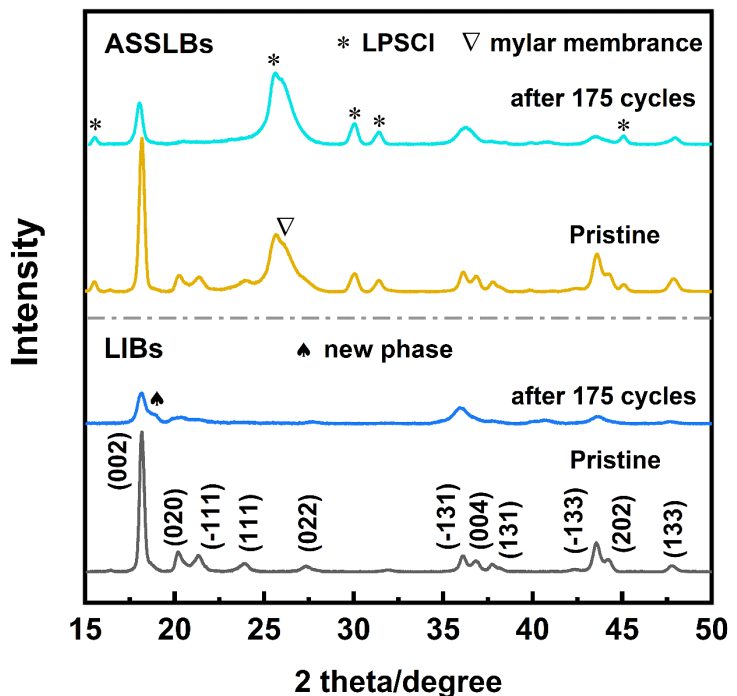


Fig. S15 Ex-situ XRD patterns of LRO in ASSLBs and LIBs.

Table S1. A detailed comparison of the electrochemical performance of the LRO with currently commercialized layered oxide cathode at the state-of-the-art ASSLBs reported in the literatures, including battery designs and operating conditions.

Ref.	Coating/cathode	Electrolyte	Voltage range (V vs Li/Li ⁺)	Current density (mA g ⁻¹)	Initial capacity (mAh g ⁻¹)	cycle number	Retention rate
[¹]	Li ₂ WO ₄ /LiCoO ₂	Li ₆ PS ₅ Cl	2.8-4.2	16	142	100	93%
[²]	LiZr ₂ (PO ₄) ₃ /LiCoO ₂	Li ₆ PS ₅ Cl	2.6-4.5	28	143.3	100	95.5%
[³]	Li ₂ CoTi ₃ O ₈ /LiCoO ₂	Li ₁₀ GeP ₂ S ₁₂	2.1-4.5	30	180	100	73.3%
[⁴]	bare/ SC-NCA811	Li ₆ PS ₅ Cl	3.0-4.3	20	191	200	63.1%
[⁴]	bare/ PC-NCA811	Li ₆ PS ₅ Cl	3.0-4.3	20	164	200	20.6%
[⁵]	bare/ rod-shaped-NCM75	Li ₆ PS ₅ Cl	3.0-4.3	100	194	200	79.1%
[⁶]	bare/ SC-NCM811	Li ₁₀ SnP ₂ S ₁₂	2.85-4.35	18	187	100	64.5%
[⁷]	bare/ SC-NCM83	Li _{9.54} Si _{1.74} P _{1.44} S _{11.7} Cl _{0.3}	2.5-4.4	100	175.5	500	85.1%
[⁸]	LiNbO ₃ /Core-shell NCA	Li ₁₀ GeP ₂ S ₁₂	2.72-4.32	60	184.1	400	89.4%
[⁹]	H-Li ₃ PO ₄ /NCM 811	Li ₁₀ GeP ₂ S ₁₂	2.7-4.5	0.2 C	163.2	300	58.9%
[¹⁰]	Al/Core-shell NCM90	Li _{9.54} Si _{1.74} P _{1.44} S _{11.7} Cl _{0.3}	2.7-4.3	200	156.8	500	96.3%
[¹¹]	LiNbO ₃ -LiCoO ₂ /NCM 811	Li _{9.54} Si _{1.74} P _{1.44} S _{11.7} Cl _{0.3}	2.7-4.38	60	182.4	585	80%
[¹²]	Li ₂ SiO _x /S-NMC	Li ₆ PS ₅ Cl	2.4-4.2	67	145	1000	62.9%
[¹³]	LiNbO ₃ / NCM	Li ₆ PS ₅ Cl	2.8-4.2	32.3	168	2000	93%
[¹⁴]	LiNbO ₃ /NCA	Li _{2.96} P _{0.98} S _{3.92} O _{0.06}	2.8-4.2	13.3	165.7	50	93.45%
This work	bare/Li ₂ RuO ₃	Li ₆ PS ₅ Cl	2.0-4.3 V	20	230	100	98%
This work	bare/Li ₂ RuO ₃	Li ₆ PS ₅ Cl	2.0-4.3 V	200	203	1000	90%

Table S2. Phase equilibria and decomposition energies of the LPSCl-LRO, LPSCl-LCO and LPSCl-NCM interfaces. x is the Molar Fraction of LPSCl in $[x \cdot \text{LPSCl} + (1-x) \cdot \text{LRO/LCO/NCM}]$

Celectrode	State	x	Phase equilibria	ΔH_D (eV/atom)
Chemical reaction				
LRO	Full-lithiated	0.429	$\text{Li}_3\text{PO}_4 \text{ Li}_2\text{S} \text{ RuS}_2 \text{ LiCl}$	-0.404
	Electrochemical reaction			
	At LRO μ_{Li}	0.314	$\text{Li}_2\text{SO}_4 \text{ Li}_3\text{PO}_4 \text{ RuS}_2 \text{ LiCl}$	-0.819
		0.413	$\text{S}_8\text{O} \text{ Li}_3\text{PO}_4 \text{ RuS}_2 \text{ LiCl}$	-0.759
		0.963	$\text{S}_8\text{O} \text{ Li}_3\text{PS}_4 \text{ RuS}_2 \text{ LiCl}$	-0.224
Chemical reaction				
LCO	Full-lithiated	0.024	$\text{Li}_{10}\text{Co}_4\text{O}_9 \text{ Li}_3\text{PO}_4 \text{ Li}_2\text{SO}_4 \text{ CoO} \text{ LiCl}$	-0.125
		0.15	$\text{Li}_6\text{Co}_4\text{O}_4 \text{ Li}_3\text{PO}_4 \text{ Co}_9\text{S}_8 \text{ Li}_2\text{SO}_4 \text{ LiCl}$	-0.298
		0.172	$\text{Li}_2\text{O} \text{ Li}_3\text{PO}_4 \text{ Co}_9\text{S}_8 \text{ Li}_2\text{SO}_4 \text{ LiCl}$	-0.317
		0.258	$\text{Li}_3\text{PO}_4 \text{ Li}_2\text{S} \text{ Co}_9\text{S}_8 \text{ Li}_2\text{SO}_4 \text{ LiCl}$	-0.363
		0.314	$\text{Li}_3\text{PO}_4 \text{ Li}_2\text{S} \text{ Li}_2\text{SO}_4 \text{ Co}_3\text{S}_4 \text{ LiCl}$	-0.361
		0.333	$\text{Li}_3\text{PO}_4 \text{ Li}_2\text{S} \text{ Co}_2\text{S}_3 \text{ LiCl}$	-0.356
	Electrochemical reaction			
	At LCO μ_{Li}	0.04	$\text{CoO} \text{ Li}_2\text{SO}_4 \text{ Li}_3\text{PO}_4 \text{ LiCl}$	-0.271
		0.188	$\text{Co}_9\text{S}_8 \text{ Li}_2\text{SO}_4 \text{ Li}_3\text{PO}_4 \text{ LiCl}$	-0.585
		0.234	$\text{Co}_3\text{S}_4 \text{ Li}_2\text{SO}_4 \text{ Li}_3\text{PO}_4 \text{ LiCl}$	-0.599
		0.25	$\text{Co}_2\text{S}_3 \text{ Li}_2\text{SO}_4 \text{ Li}_3\text{PO}_4 \text{ LiCl}$	-0.597
		0.333	$\text{Co}_2\text{S}_3 \text{ Li}_2\text{S} \text{ Li}_3\text{PO}_4 \text{ LiCl}$	-0.576
Chemical reaction				
NCM	Full-lithiated	0.277	$\text{LiMnO}_2 \text{ Co}_9\text{S}_8 \text{ Li}_2\text{SO}_4 \text{ Ni}_3\text{S}_2 \text{ Li}_2\text{O} \text{ LiCl} \text{ Li}_3\text{PO}_4$	-0.299
		0.39	$\text{LiMnO}_2 \text{ Co}_9\text{S}_8 \text{ Li}_2\text{SO}_4 \text{ Ni}_3\text{S}_2 \text{ Li}_2\text{S} \text{ LiCl} \text{ Li}_3\text{PO}_4$	-0.337
		0.433	$\text{Co}_9\text{S}_8 \text{ Li}_2\text{SO}_4 \text{ MnO} \text{ Ni}_3\text{S}_2 \text{ Li}_2\text{S} \text{ LiCl} \text{ Li}_3\text{PO}_4$	-0.349
		0.489	$\text{Li}_2\text{SO}_4 \text{ Co}_2\text{Ni}_3\text{S}_4 \text{ MnO} \text{ Ni}_3\text{S}_2 \text{ Li}_2\text{S} \text{ LiCl} \text{ Li}_3\text{PO}_4$	-0.357

		0.51	<chem>Li2SO4 Co(NiS2)2 Co2NiS4 MnO Li2S LiCl Li3PO4</chem>	-0.359
		0.597	<chem>Li(MnS2)2 Li2SO4 Co(NiS2)2 Co2NiS4 Li2S LiCl Li3PO4</chem>	-0.363
		0.6	<chem>Li(MnS2)2 MnS2 Co(NiS2)2 Co2NiS4 Li2S LiCl Li3PO4</chem>	-0.364
Electrochemical reaction				
At NCM μ Li		0.319	<chem>MnO Ni3S2 Co9S8 Li2SO4 Li3PO4 LiCl</chem>	-0.552
		0.374	<chem>MnO Co2NiS4 Ni3S2 Li2SO4 Li3PO4 LiCl</chem>	-0.582
		0.395	<chem>MnO Co2NiS4 Co(NiS2)2 Li2SO4 Li3PO4 LiCl</chem>	-0.592
		0.507	<chem>Co2NiS4 Co(NiS2)2 Li2SO4 MnS2 Li3PO4 LiCl</chem>	-0.626
		0.6	<chem>Co2NiS4 Co(NiS2)2 MnS2 Li3PO4 LiCl Li2S</chem>	-0.591

References

1. Z. Sun, Y. Lai, N. lv, Y. Hu, B. Li, S. Jing, L. Jiang, M. Jia, J. Li, S. Chen and F. Liu, *Adv. Mater. Interfaces*, 2021, **8**, 2100624-2100632.
2. L. Wang, X. Sun, J. Ma, B. Chen, C. Li, J. Li, L. Chang, X. Yu, T. S. Chan, Z. Hu, M. Noked and G. Cui, *Adv. Energy Mater.*, 2021, **11**, 2100881-2100891.
3. C. Wang, J. Liang, Y. Zhao, M. Zheng, X. Li and X. Sun, *Energy Environ. Sci.*, 2021, **14**, 2577-2619.
4. Y. Han, S. H. Jung, H. Kwak, S. Jun, H. H. Kwak, J. H. Lee, S. T. Hong and Y. S. Jung, *Adv. Energy Mater.*, 2021, **11**, 2100126-2100141.
5. S. H. Jung, U. H. Kim, J. H. Kim, S. Jun, C. S. Yoon, Y. S. Jung and Y. K. Sun, *Adv. Energy Mater.*, 2019, **10**, 1903360-1903372.
6. X. Liu, B. Zheng, J. Zhao, W. Zhao, Z. Liang, Y. Su, C. Xie, K. Zhou, Y. Xiang, J. Zhu, H. Wang, G. Zhong, Z. Gong, J. Huang and Y. Yang, *Adv. Energy Mater.*, 2021, **11**, 2003583-2003594.
7. W. Jiang, X. Fan, X. Zhu, Z. Wu, Z. Li, R. Huang, S. Zhao, X. Zeng, G. Hu, B. Zhang, S. Zhang, L. Zhu, L. Yan, M. Ling, L. Wang and C. Liang, *J. Power Sources*, 2021, **508**, 230335-230345.
8. X. Li, M. Liang, J. Sheng, D. Song, H. Zhang, X. Shi and L. Zhang, *Energy Storage Mater.*, 2019, **18**, 100-106.
9. S. Deng, X. Li, Z. Ren, W. Li, J. Luo, J. Liang, J. Liang, M. N. Banis, M. Li, Y. Zhao, X. Li, C. Wang, Y. Sun, Q. Sun, R. Li, Y. Hu, H. Huang, L. Zhang, S. Lu, J. Luo and X. Sun, *Energy Storage Mater.*, 2020, **27**, 117-123.
10. X. Li, Y. Sun, Z. Wang, X. Wang, H. Zhang, D. Song, L. Zhang and L. Zhu, *Electrochim. Acta*, 2021, **391**, 138917-138927.
11. X. Li, Q. Sun, Z. Wang, D. Song, H. Zhang, X. Shi, C. Li, L. Zhang and L. Zhu, *J. Power Sources*, 2020, **456**, 227997-228007.
12. D. Cao, X. Sun, Y. Li, A. Anderson, W. Lu and H. Zhu, *Adv. Mater.*, 2022, **24**, 2200401-2200414.
13. S. Liu, L. Zhou, J. Han, K. Wen, S. Guan, C. Xue, Z. Zhang, B. Xu, Y. Lin, Y. Shen, L. Li and C. W. Nan, *Adv. Energy Mater.*, 2022, 2200660-2200669.
14. N. Ahmad, S. Sun, P. Yu and W. Yang, *Adv. Funct. Mater.*, 2022, 2201528-2201541.